Foto by Christian Ammering

Modelling Swelling Rock Behaviour in Tunnelling

Bert Schädlich & Helmut F. Schweiger, Institute for Soil Mechanics and Foundation Engineering, Graz University of Technology, Graz, Austria
Thomas Marcher, ILF Consulting Engineers, Innsbruck, Austria

Although a great amount of practical experience has been gained in the last decades, tunnel design in swelling rock is still a very challenging task, as the recent examples of the Engelbergtunnel in southern Germany and the Chienbergtunnel in Switzerland demonstrate. Reliable prediction of swelling pressures and swelling deformations especially in anhydritic rock is extremely difficult due to the heterogeneity of the material and the complexity of the involved transport mechanisms. However, modern design codes and engineering practice demand capacity checks for tunnel linings, which usually can only be provided by numerical analysis with an appropriate constitutive model. Such a constitutive swelling model, which adds swelling strains in dependence on the stress level and accounts for the time dependent evolution of swelling, has been implemented for Plaxis. This article compares the results of a numerical back analysis with this model to in-situ measurements, using swelling parameters derived from laboratory swelling tests.

"Swelling rocks" are geomaterials which increase in volume if water is allowed to infiltrate. The most prominent rock types exhibiting swelling behaviour are certain types of claystone and anhydrite-bearing rocks, which can be commonly found in northern Switzerland and southern Germany. Tunnelling in such materials is notoriously difficult: If a flexible invert lining is installed, large invert heave evolves after tunnel excavation. In case these deformations are prevented by a rigid support concept, large swelling pressures may develop at the tunnel lining. It is well known that swelling deformations – at least in claystone – reduce with the logarithm of stress, and that swelling deformations can be completely suppressed by sufficiently high pressure. The chemical processes in anhydrite swelling, on the other hand, are completely different, and the semi-logarithmic relationship between swelling strains and stress level (Grob 1972) is not universally accepted for these materials. Evolution of swelling with time in both claystone and anhydrite depends on the availability of water, which is governed by the permeability of the material, layering of the subsoil and the amount of water recharge. As some of these factors relate to characteristics of the specific boundary value problem rather than

the material itself, parameters determining the time-swell behaviour cannot be transferred from laboratory tests to large-scale problems.

Constitutive model
The constitutive model used in this paper has been implemented by T. Benz (NTNU Norway) as a user-defined soil model for PLAXIS. The model employs four parameters for strength and stiffness and three parameters for swelling. ϕ' and c' are the well-known Mohr-Coulomb friction angle and cohesion, E and ν are the isotropic elastic Young's modulus and Poisson's ratio, respectively. Cross-anisotropic elasticity can also be considered but is not used in this study. The meaning of the swelling parameters is shown in Figure 1 and Figure 2. The maximum swelling pressure σ_{q0} is the axial stress beyond which no swelling occurs, the swelling potential k_q gives the inclination of the swelling curve in semi-logarithmic scale and the parameter η_q is related to the time until the final swelling strain has developed (Wittke & Wittke 2005). Cross-anisotropic swelling can be considered in the model, but again this feature is not used here.

$$\varepsilon_i^{q(t=\infty)} = -k_{qi} \cdot \log_{10}\left(\frac{\sigma_i}{\sigma_{q0i}}\right) \quad (1)$$

If necessary the time-swell behaviour can be related to elastic and plastic volumetric strains, ε_v^{el} and ε_v^{pl}, by using parameters A_{el} and A_{pl} to define the time swelling parameter η_q:

$$\eta_q(t) = 1 / \left(A_0 + A_{el} \cdot \varepsilon_v^{el} + A_{pl} \cdot \varepsilon_v^{pl}\right) \quad (2)$$

Positive volumetric strains (loosening of the material) result in faster approach of the final swelling strain, while negative volumetric strains delay or may even stop the evolution of the swelling strains. This approach accounts for the dependency of the swelling rate on the penetration rate of water.

Construction of the Pfändertunnel
The 6.7 km long first tube of the Pfaendertunnel near Bregenz (Austria) was constructed in 1976-1980 according to the principles of the New Austrian Tunnelling method (NATM). While top heading and bench excavation were carried out without major difficulties, significant invert heave of up to 30 cm was observed after about 75% of the tunnel length was excavated. These observations lead to detailed laboratory investigations of the swelling characteristics of the Pfaenderstock material, an extensive monitoring program and to the installation of additional anchors in the tunnel invert.

Laboratory swelling tests

The Pfaenderstock consists of various layers of sandstone, conglomerate, claystone and marl, which are summarized as upper freshwater molasse. The marl (claystone) layers were identified as the rock type causing the swelling due to their high content of Montmorillonite (Weiss et al. 1980). Czurda & Ginther (1983) distinguished between undisturbed molasse marl (series A, Figure 4) and the fault zone material (series B, Figure 5). Series A samples showed

higher swelling potential, but lower maximum swelling pressures than the samples of series B. This notable difference was attributed to relaxation and swelling of the series B samples before the samples could be tested.

For the back analysis two swelling parameter sets are considered, which represent the upper and lower boundary of the test results. The time swelling parameters A_0, A_{el} and A_{pl} are calibrated to match the in situ time-swelling curve.

Numerical model and material parameters

The 2D finite element model used in this study is shown in Figure 6. Tunnel geometry and basic material parameters of the marl layer (E = 2.5 GPa,

ϕ' = 34°, c' = 1000 kPa) have been taken from John et al. (2009). Tunnel overburden is ~200 m above the tunnel crown, which is representative of the cross section at km 5+373. Linear elastic plate elements are used for the shotcrete lining, with E = 7.5 GPa for the young and E = 15 GPa for the cured shotcrete. The final concrete lining is modelled with volume elements assuming linear elastic behaviour and a stiffness of E = 30 GPa. The final lining thickness varies between 50 cm at the invert and 25 cm at the crown.

Swelling parameters are listed in Table 1. Sets 1a, 1b and 2a only employ A_0 for the time dependency of swelling, while in set 2b evolution of swelling with time is entirely governed by elastic volumetric strains.
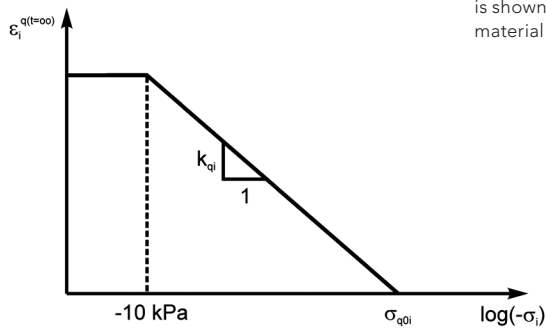

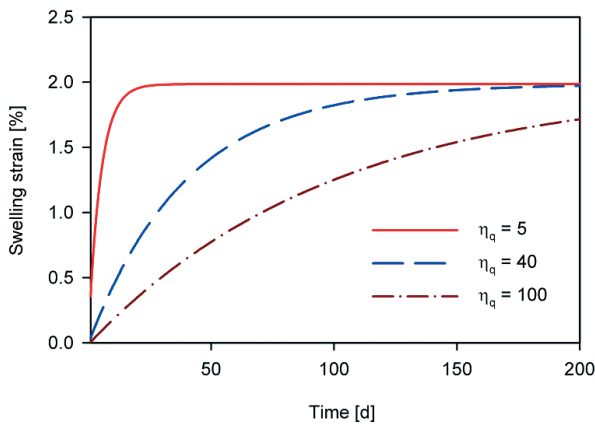*Fig. 1: Semi-logarithmic swelling law (Grob 1972)*

Figure 2: Influence of η_q on evolution of swelling strains
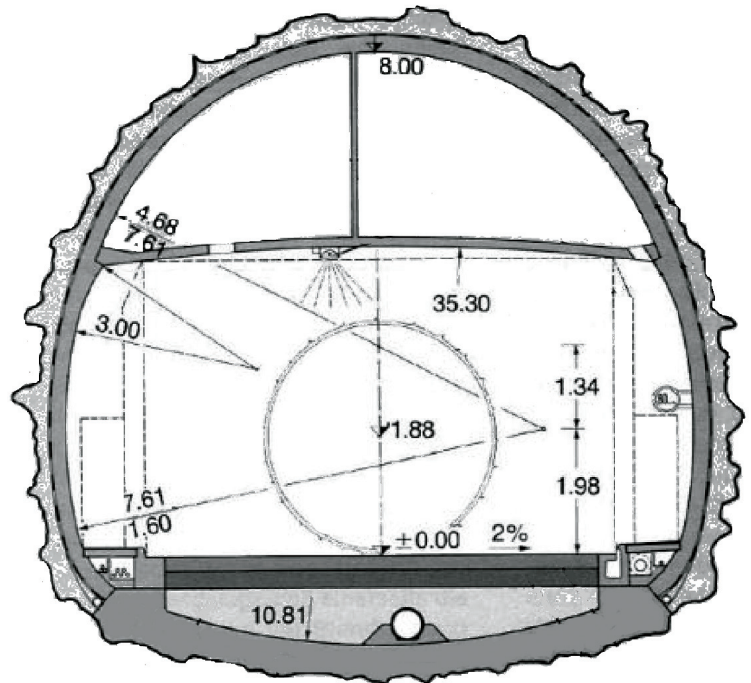

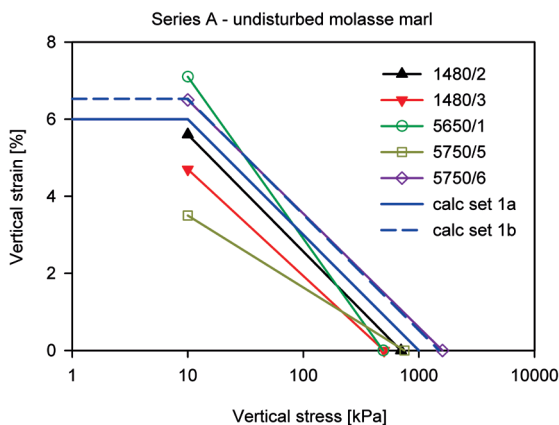*Figure 3: Pfaendertunnel cross section 1st tube (after John & Pilser 2011)*

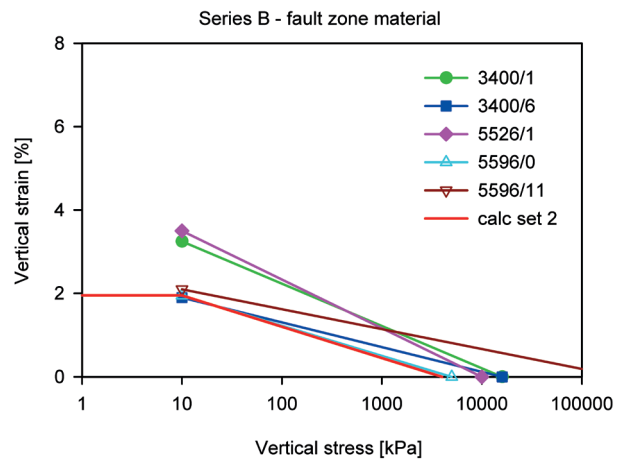*Figure 4: Swelling test results, series A*

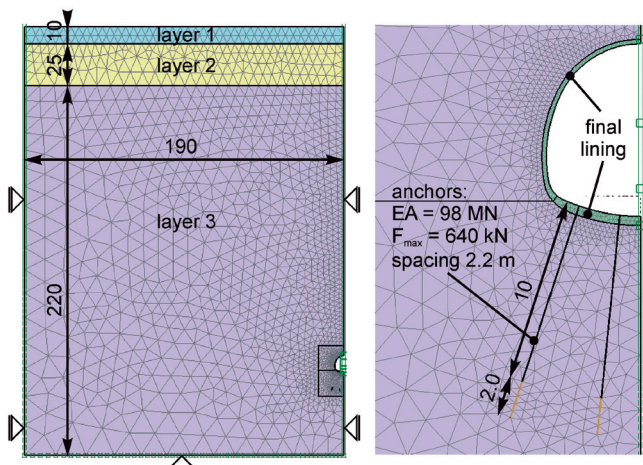*Figure 5: Swelling test results, series B*

Figure 6: Finite element model (dimensions in m)

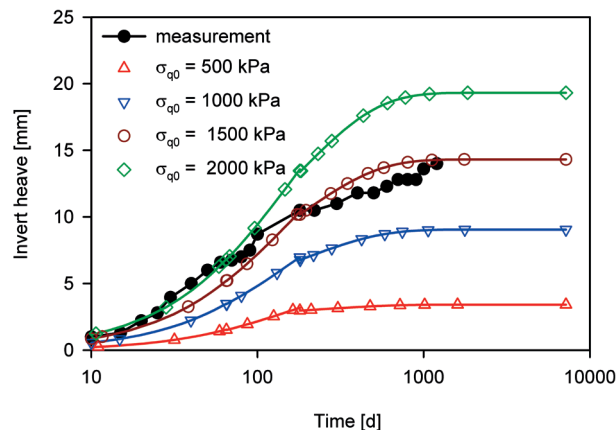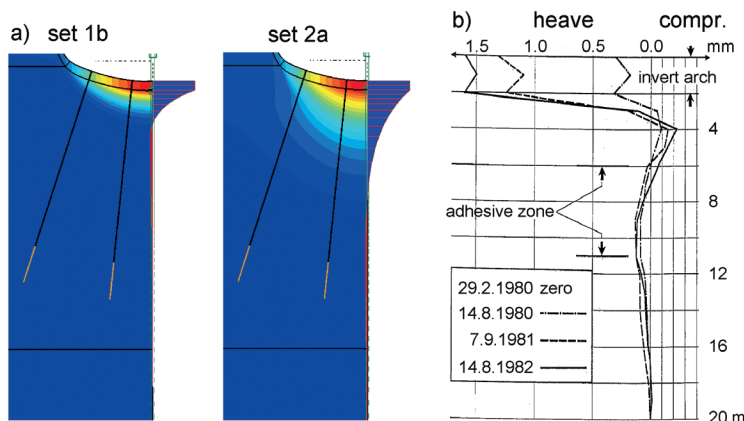
Figure 7: Development of invert heave with time

Figure 8: Profile of vertical displacements, a) numerical analysis at t = 7180 d, b) measurements km 5+820 (after John 1982)
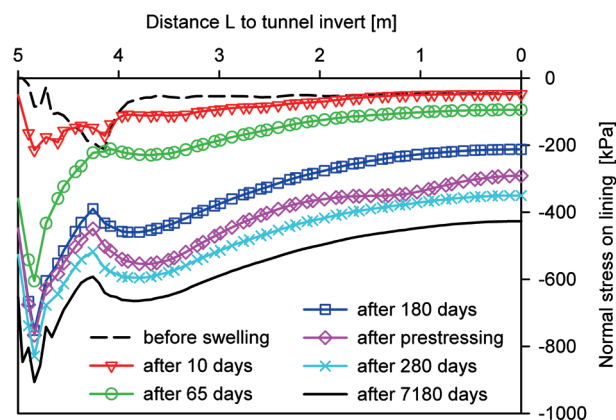

Figure 9: Development of pressure on the lining (set 1b)

Parameter	Set 1a	Set 1b	Set 2a	Set 2b
Swelling potential k_q [%]	3.0	3.0	0.75	0.75
Max. swelling stress σ_{q0} [kPa]	1000	1500	4000	4000
A_0	$5.0e^{-3}$	$2.5e^{-3}$	$3.0e^{-3}$	0.0
A_{el}	0.0	0.0	0.0	9.0
A_{pl}	0.0	0.0	0.0	0.0

Table 1: Swelling parameters

Calculation phases

After top heading / invert excavation (assuming pre-relaxation factors of 75% and 37.5%, respectively), the concrete invert arch is installed. Swelling is confined in the model to an area of 15 m x 15 m below the tunnel invert. After a swelling phase of 65 days, the final lining is activated, followed by another swelling phase of 115 days. John (1982) reported that the decision on invert anchoring and pre-stressing was based on the swell heave deformations observed up to this point. In the cross section considered here this resulted in an anchor pattern of 2.2 m spacing.

Evolution of invert heave with time

Figure 9 compares the time-swelling curves calculated with the different parameter sets with the measured invert heave in km 5+373. The measurements plot close to a straight line in logarithmic time scale, which cannot be reproduced exactly by the exponential approach employed in the model. The match with the measured invert heave is, however, sufficient from a practical point of view.

Set 1a delivers too little invert heave (10mm), and the development of deformations completely

stops after activating the prestressed anchors. Increasing the maximum swelling stress by 50% (set 1b) yields ~50% more deformation and a better match with the measurements. While such a significant influence may be expected, it should be noted that experimental results for these two sets plot so close to each other that either of the two parameter sets appears justified (Figure 4). Surprisingly, sets 2a and 2b – which represent much smaller free-swell deformations – deliver more invert heave than sets 1a and 1b. This is a result of the higher maximum swelling stress in sets 2a and 2b, which activates swelling in deeper rock layers, yet with a small swelling potential. Swelling deformations are thus more widely distributed with set 2a and 2b.

Modelling the evolution of swelling with time entirely in dependence on elastic volumetric strains (set 2b) results in a slightly more prolonged time-swell-curve than using a constant value of A_0 (set 2a). In set 2b the rate of swelling does not only decrease due to the convergence with the final swelling strain, but also due to negative elastic volumetric strains. The large positive volumetric strains after tunnel excavation are gradually reduced in the swelling phases by the increasing swelling pressure.
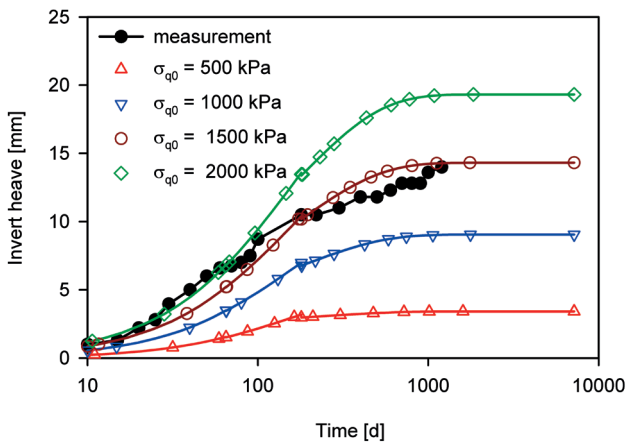
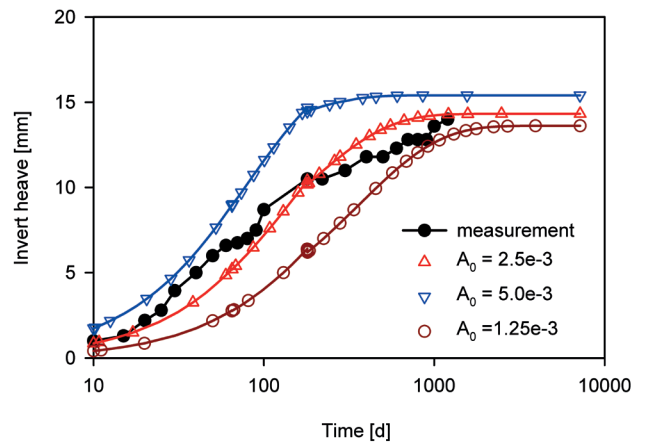Figure 10: Variation of maximum swelling stress

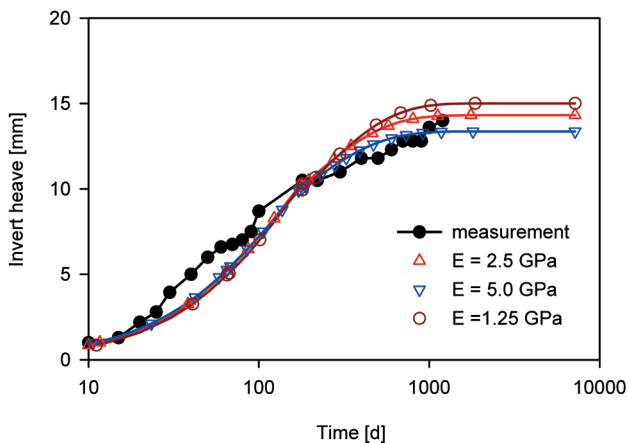Figure 11: Variation of time swelling parameters (set 1b)

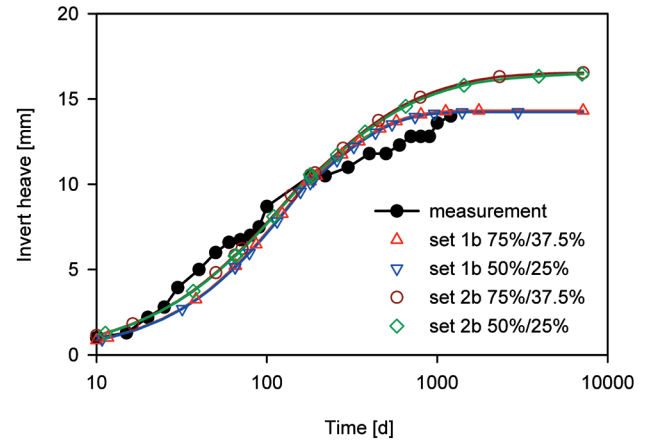
Figure 12: Variation of rock stiffness (set 1b)

Figure 13: Variation of stress pre-relaxation

Distribution of swelling strains over depth

The proportion of the rock mass which is affected by swelling depends primarily on the maximum swelling stress. For set 1b (σ_{q0} = 1500 kPa) the swelling zone is confined to about 2 m below the tunnel invert, which matches well with the sliding micrometer measurements in the neighbouring cross section km 5+820 (Figure 8). The swelling zone with set 2a (σ_{q0} = 4000 kPa) is much deeper due to the higher maximum swelling pressure, even though similar invert heave is obtained with both parameter sets. These results indicate that the maximum in situ swelling pressure is rather in the range of 1000-2000 kPa than close to the in-situ stresses.

Swelling pressure

Figure 9 shows the distribution of swelling pressure on the tunnel invert lining for different stages in time for parameter set 1b. The circumferential distance L is measured from the tunnel invert, such that L = 0 m is directly at the invert and L = 5 m is the end of the swelling area. No pressure measurements are available.

Due to the stiffer support provided to the tunnel lining at the sides of the tunnel, the maximum

swelling pressure does not occur at the tunnel invert but at a distance of ~3.8 m.

Anchor prestressing increases the normal stress on the lining by about 90 kPa. The difference to the distributed prestressing force of (0.8*640 kN / 2.2 m / 2.2. m) = 106 kN/m² is a result of the already closed final lining, which distributes part of the applied load in circumferential direction. Comparing the increase in pressure to the swelling line of set 1b at 200-300 kPa (Figure 4) explains the limited influence of prestressing in the numerical calculations. Even though anchor prestressing increases the pressure by ~45%, reduction of final swelling strain is only about 18% due to the semi-logarithmic swelling law. Additionally, the effect of prestressing diminishes rapidly with increasing distance to the tunnel, and the deeper rock layers remain virtually unaffected.

Variation of maximum swelling pressure

The calculated invert heave is notably sensitive to the maximum swelling pressure σ_{q0} assumed in the numerical analysis. As the variation of this parameter in the laboratory swelling tests is rather large– albeit concealed by the logarithmic stress scale – σ_{q0} has been varied from 500 kPa

to 2000 kPa (A_0 = 2.5e^{-3}). Results indicate a linear increase of invert heave with σ_{q0} (Figure 10). This is primarily the result of the increasing depth of the swelling zone below the tunnel invert (Figure 8), and not so much due to higher swelling strains directly underneath the tunnel invert.

Influence of other material parameters

The influence of other material parameters on swelling deformations is limited. As expected, the time swelling parameter A_0 has a notable influence on the evolution of swelling deformations, but not on final deformations (Figure 11). Varying the elastic rock stiffness had virtually no effect on swelling deformations after tunnel excavation (Figure 12), but naturally changed deformations during tunnel excavation. Variation of the 2D pre-relaxation factors – which in most practical cases are an educated guess rather than a thoroughly derived parameter – also had no notably influence on swelling deformation (Figure 13). As no temporary invert lining was installed after top heading excavation, stresses in the rock mass at the tunnel invert drop to ~0 during tunnel excavation, independent of the pre-relaxation factors applied in the excavation phases.

Concluding remarks

This article presented the results of a back analysis of measured swelling deformations in the Pfaendertunnel (Austria). A constitutive model based on Grob's swelling law and exponential convergence with final swelling strains over time was used for the numerical calculations. Input swelling parameters were derived from laboratory swelling tests. Due to the large variation of laboratory test results, the sensitivity of model predictions on the input swelling parameters was investigated.

Different sets of swelling potential k_q and maximum swelling stress σ_{q0} delivered very similar swelling deformations at the tunnel lining, as increasing σ_{q0} is roughly equivalent to increasing k_q. However, good match with the measured displacement profile below the tunnel invert was only obtained with σ_{q0} = 1500 kPa, which represents the upper edge of the experimental results on undisturbed molasse marl. Using higher values of σ_{q0} (and lower values of k_q) delivers too large swelling zones. The invert heave measurements plot close to a straight line in logarithmic time scale, which cannot be exactly reproduced by the exponential approach of the constitutive model. The match with the measured evolution of swelling, however, is sufficient from a practical point of view.

References

• Czurda, K. A., and Ginther, G. (1983) "Quellver-halten der Molassemergel im Pfänderstock bei Bregenz, Österreich", Mitt. österr. geolog. Ges., 76, pp. 141-160.
• Grob, H. (1972) "Schwelldruck im Belchentun-nel", Proc. Int. Symp. für Untertagebau, Luzern, pp. 99-119.
• John, M. (1982) "Anwendung der neuen öster-reichischen Tunnelbauweise bei quellendem Gebirge im Pfändertunnel" Proc. of the 31st Geomechanik Kolloquium, Salzburg, Austria.
• John, M., Marcher, T., Pilser, G., and Alber, O. (2009) "Considerations of swelling for the 2nd bore of the Pfändertunnel", Proc. of the World Tunnel Congress 2009, Budapest, Hungary, pp. 50-61.
• John, M., and Pilser, G. (2011) "Criteria for selecting a tunnelling method using the first and the second tube of the Pfänder tunnel as example", Geomechanics and Tunnelling, 4(11), pp. 527-533.
• Weiss, E. H., Müller, H. M., Riedmüller, G., and Schwaighofer, B. (1980) "Zum Problem quellfähiger Gesteine im Tunnelbau", Geolog. Paläont. Mitt. Innsbruck, 10(5), pp. 207-210.
• Wittke, W., and Wittke, M. (2005) "Design, con-struction and supervision of tunnels in swelling rock", Proc. 31st ITA World Tunnelling Congress 2005, pp. 1173-1178.